Industrial Application of RANS Modelling: Capabilities and Needs

Farzin Shakib
VP. CFD Technology
2685 Marine Way, Suite 1421, Mountain View, CA 94043
fshakib@altair.com

And
David Corson
Program Manager, AcuSolve
Clifton Park, NY 12065
dcorson@altair.com

And
Rajeev Jaiman
Rajeev_jaiman@acusim.com

Abstract

This article focuses on the current capabilities of Reynolds-Averaged Navier-Stokes (RANS) turbulence modelling and its application to industrial flows. The experiences discussed here are the culmination of over 15 years of commercial application of the Galerkin/Least-Squares Finite Element Method and RANS turbulence modelling approach. The objective of this article is to provide a brief review of turbulence modelling, then illustrate how industrial users are successfully leveraging RANS techniques in production environments. Applications of increasing complexity involving adverse pressure gradients, separation and complex 3-D systems are presented to illustrate the strengths of RANS and unsteady RANS (URANS) modelling. Results are also presented to draw attention to some of the limitations of RANS technology for industrial applications of specific interest. Finally, motivation for continuing research in the field of RANS modelling is provided.

Keywords: industrial turbulent flows; Spalart-Allmaras RANS model; Galerkin/Least-Squares; finite element; massive separation; transition; adverse-pressure gradient; AcuSolve

1.0 Introduction

A complete and accurate time-dependent solution of the discretised Navier-Stokes equations for high Reynolds number turbulent flows in complex geometries continues to be unobtainable using current computing resources. Unfortunately, recent estimates based on trends in the computing industry indicate that this will continue to be the case for years to come (Spalart et al. 1997, Spalart 2000). In light of this fact, CFD practitioners are forced to make simplifying assumptions about the flows they wish to model in order to make them computationally tractable. Current practices for modelling turbulent flow presents analysts with two primary methods of reducing the cost of solving the full set of Navier-Stokes equations: Reynolds averaging and filtering (Wilcox 2000). Both of these approaches involve a transformation of the Navier-Stokes equations in such a manner that all or part of the turbulent flow structure is modelled and not resolved explicitly. The most common approach to turbulence modelling utilises the Reynolds averaging procedure (Pope 2000) to

arrive at the Reynolds-Averaged Navier- Stokes (RANS) equations. This operation eliminates the need to resolve the turbulent structures of a flow field, and instead attempts to model the diffusive effect of these structures on the time averaged flow. An alternative approach to Reynolds averaging involves a filtering operation to eliminate only the small scale turbulent structures. Large Eddy Simulations (LES) integrate these filtered equations in time to provide detailed flow field information containing an explicit, time accurate representation of the large scale turbulent motions (Moin and Kim 1982, Moin 1984). Various LES closures are available including the classical fixed coefficient Smagorinsky model (Smagorinsky 1963), the dynamic model (Germano et al. 1991, Carati et al. 1995), and the Variational Multi-Scale (VMS) model (Hughes et al. 2000). LES represents a reduced order modelling approach in relation to the Reynolds averaging operation, but also represents a significant increase in computational cost. In addition to these two primary approaches to turbulence modelling, a number of hybrid approaches have evolved in recent years that attempt to combine the benefits of LES and RANS (Spalart et al. 1997, Batten et al. 2002, Girimaji et al. 2003, Menter et al. 2003, Spalart et al. 2006). Hybrid RANS/LES methods, commonly referred to as Detached Eddy Simulation (DES) models, resolve large scale turbulent motions in separated flow regions, and revert to the use of the unsteady RANS equations in attached boundary layers. These methods have been successfully applied for a variety of flows (Breuer et al. 2003, Slimon 2003, Lyons et al. 2007). However, as with LES, the hybrid approaches have a significant increase in computational cost when compared to steady RANS methods.

All of the approaches described above introduce additional terms into the Navier-Stokes equations. This gives rise to the well-known closure problem of turbulence. It is necessary to develop auxiliary relations to enable a solution of the equations. For LES and hybrid approaches, the closure method requires a transient solution approach and high levels of mesh resolution to achieve accurate results. In the case of RANS modelling, closure is typically achieved through the solution of one or more partial differential equations. These additional equations allow users to directly simulate the time averaged flow without the need to perform a transient simulation. For applications where the transient behaviour of the flow is of interest, the RANS closure may be used in an unsteady mode to provide a simulation technique with less demanding grid and time stepping requirements than LES and DES. Both utilisations of RANS closures (steady and unsteady) represent significant computational savings over the alternatives. This is of critical importance to industrial users. In addition to providing computational efficiency, RANS modelling has benefited from decades of academic research that has led to the development of very advanced closures. Although a universal model of turbulence still eludes researchers, these advanced models give industrial users powerful tools for use in their design and analysis processes. In this article, a brief description of the numerical methods used in the flow solver is presented, followed by a summary of the use of RANS and URANS modelling in Section 3. In Section 4, some current applications that present significant demands to the RANS methodology are discussed, and the motivation for continued research in RANS modelling is presented in the conclusion.

2.0 Numerical method

In this work, the Navier-Stokes equations are solved using AcuSolveTM, a commercially available software package based on the Galerkin/Least-Squares (GLS) finite element method (Hughes et al. 1989, Shakib et al. 1991). AcuSolve is a general purpose CFD flow solver that is used in a wide variety of applications and industries such as automotive, off-shore engineering, electronics cooling, chemical mixing, bio-medical, consumer products, national laboratories and academic research. The flow solver is architected for parallel execution on shared and distributed memory computer systems and provides fast and efficient transient and steady state solutions for standard unstructured element topologies.

The GLS formulation provides second order accuracy for spatial discretisation of all variables and utilises tightly controlled numerical diffusion operators to obtain stability and maintain accuracy. In addition to satisfying conservation laws globally, the formulation implemented in AcuSolve ensures local conservation for individual elements. Equal-order nodal interpolation is used for all working variables, including pressure and turbulence equations. The semidiscrete generalised-a method (Jansen et al. 2000) is used to integrate the equations in time for transient simulations. The resultant system of equations is solved as a fully coupled pressure/velocity matrix system using a pre-conditioned iterative linear solver. The iterative solver yields robustness and rapid convergence on large unstructured industrial meshes even when high aspect ratio and badly distorted elements are present. For applications involving species transport, the scalar equations are solved segregated from the Navier-Stokes system. When simulating thermal transport, AcuSolve offers the option of solving the enthalpy conservation equation in a segregated fashion or fully coupled as a mass, momentum and enthalpy matrix system. The one-equation Spalart-Allmaras (SA) turbulence model is used in all RANS results presented in this paper (Spalart and Allmaras 1992). The turbulence equation is solved segregated from the flow equations using the GLS formulation. A stable linearisation of the source terms is constructed to yield a robust and efficient implementation of the model.

3.0 Applications of RANS modelling

The presence of CFD in industry has steadily increased in the past decade, primarily due to advances in hardware and software technology. The success of RANS modelling has also played a critical role in this process, providing the enabling technology that most industrial simulations are based on. In the following discussion, representative AcuSolve RANS results are presented, ranging in complexity from very simple to very demanding applications.

3.1. Attached boundary layer flows

Attached boundary layer flows are perhaps the most natural application of RANS modelling. Most RANS models are developed with this flow regime in mind, and are able to reproduce turbulent boundary layer flows well. Applications of this type are very common in industry and are encountered in the simulation of flow through piping systems, heat exchangers and electronic devices. Although many of these applications may include flow separation in some regions, the majority of the boundary layer remains attached. Such applications regularly produce accurate results for heat transfer coefficients, mean velocity profiles and pressure drops. A widely used test case to measure the performance of turbulence models for such conditions was reported in Samuel and Joubert (1974).

This case consists of a steady flat plate boundary-layer, developing under an increasingly adverse pressure gradient, as shown in **Figure 1a**. The Reynolds number based on inlet height is Re ¼ 1.7 6 106. The flow is inhibited by the pressure gradient, but no separation occurs. **Figure 1b** shows good agreement of the skin friction distribution between the RANS model and the experimental data. The figure also depicts the variation of pressure coefficient predicted by the model. The results presented are based on a thorough mesh sensitivity study and represent accurate solutions to the governing equations.

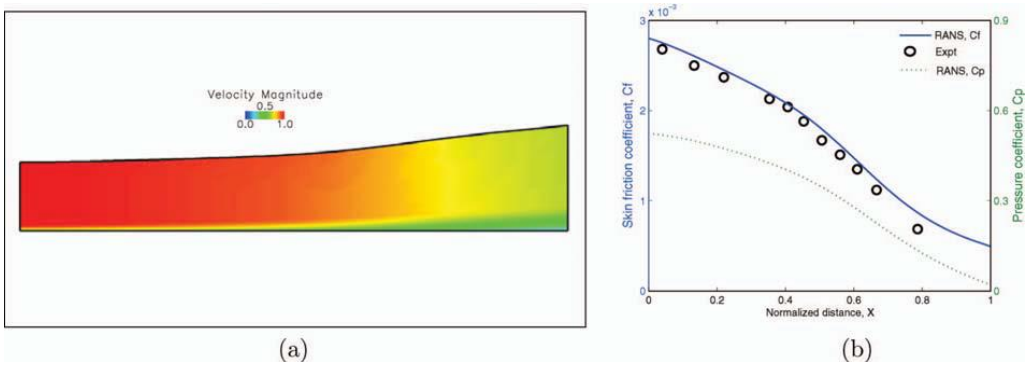

Figure 1. Steady RANS results of attached boundary layer with a mildly adverse pressure gradient: (a) contours of velocity magnitude; (b) skin friction and pressure coefficients.

Furthermore, this case is used as validation of the wall function employed by the Spalart-Allmaras model in AcuSolve, which allows users to circumvent the wall normal grid refinement required to resolve the nearwall behavior. This case utilises wall functions and illustrates the insensitivity of the wall-function to mesh construction by producing excellent results on meshes having their first nodes falling anywhere within the viscous sublayer and logarithmic layer.

3.2. Mildly separated flows

To illustrate the capabilities of RANS models for mildly separated flows, a curved solid hump embedded in a turbulent boundary layer is considered (Lyonset al. 2007). This simulation stems from a CFD validation exercise organised by the NASA Langley Research Center (Greenblatt et al. 2004). The flow on the downstream side of the hump model separates as a result of the adverse pressure gradient caused by the rapid expansion in cross sectional area. The geometry and flow field are shown in **Figures 2a,b. Figures 2c,d** present a comparison of the pressure coefficient and the skin friction distribution between the RANS model and the experimental data.

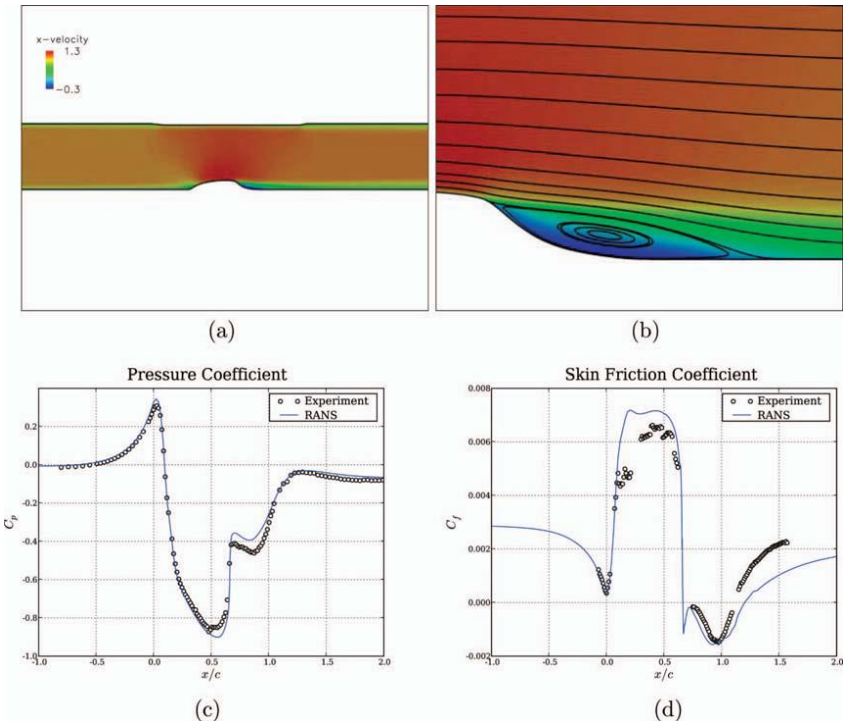

Figure 2. Steady RANS results from NASA hump model: (a) contours of stream-wise velocity; (b) streamlines showing recirculation; (c) pressure coefficient; (d) skin friction coefficient. Results courtesy of D. Lyons and Dr. L.J. Peltier of Penn State.

	RANS	Experiment
Separation	0.663	0.665
Reattachment	1.22	1.11

Table 1. Separation and reattachment points presented as non-dimensional distance (x/chord) from the leading edge of the hump.

For further analysis, **Table 1** shows that the Spalart-Allmaras model does a good job of predicting the separation location, but provides an overestimate of the reattachment point. This implies an overall underprediction of the total turbulent diffusivity in the wake of the hump. Predicting the extent of separation for this type of flow continues to challenge RANS models. Despite this shortcoming, good agreement is obtained for the pressure coefficient, with slightly worse agreement obtained for the skin friction coefficient. This validation case, although relatively simple, provides expectations to commercial users with regards to the ability of the Spalart-Allmaras RANS model to predict separation from nozzles, diffusers, pipe elbows and other contoured surfaces.

3.3. Massively separated flows

Massively separated flows give rise to turbulent structures whose size is a strong function of the geometry of the body causing the separation. RANS models are typically calibrated using attached and mildly separated flows where the turbulent structure contains a more universal and geometry independent characteristic. When steady RANS is applied to massively separated flows, the simulations may fail to converge to a steady solution. For these applications, industrial users have the option to perform a URANS analysis to investigate the flow field.

Although the theoretical basis of URANS is still debated (Shur et al. 2005), current RANS closures do have the ability to identify the presence of large scale unsteadiness when run in an unsteady mode. The flow around bluff bodies is a common test case for URANS due to the large eddies formed in the wake. **Figure 3** illustrates the transient wake structure that is predicted by the Spalart-Allmaras model for the flow over a square cylinder with rounded corners at Re ¼ 1.5 6 105. The inlet eddy viscosity is set to the kinematic viscosity to model a small amount of turbulence in the flow as it encounters the rounded leading edge of the cube. The resulting vortex shedding in the wake of the bluff body is seen in **Figure 3a** while **Figure 3b** shows the resulting oscillations in the lift and drag coefficients.

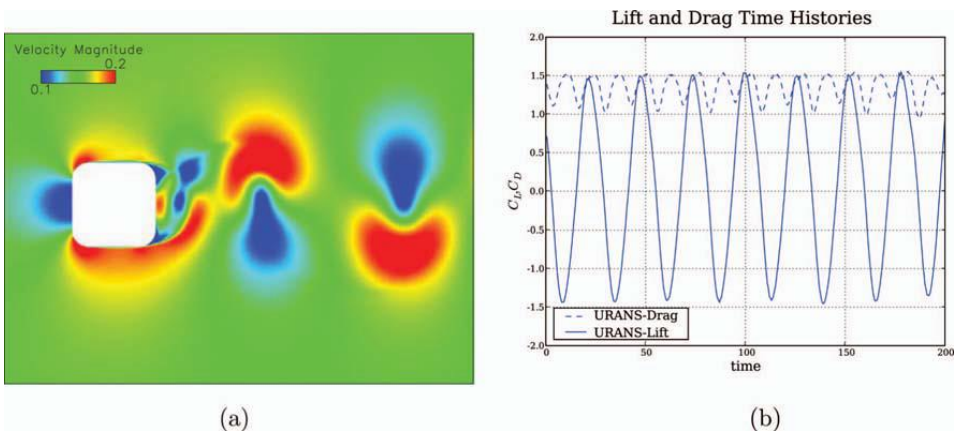

Figure 3. Unsteady RANS simulation of flow over square cylinder: (a) velocity magnitude in wake of square cylinder (b) timehistory of lift and drag coefficients.

The application of URANS to massively separated flows represents a very important class of simulations, and will be investigated in greater detail in a later section when flow over an oil platform riser is presented.

3.4. Complex 3-D Systems

The previous examples of RANS applications focused on a single flow feature (i.e. an attached boundary layer, a single region of separated flow, etc.). This is rarely the case when using CFD for industrial simulations. More often, simulations contain some combination of the previously discussed flow features in a single system. RANS and URANS are successfully employed for complex 3-D systems in many engineering fields. **Figure 4** illustrates an application of CFD in the automotive industry. In this simulation, the passenger compartment of an automobile is cooled from an initial temperature using a URANS approach with a wall-function treatment for unresolved boundary layers. The figure shows contours of temperature resulting from the simulation at three instants in time during the transient.

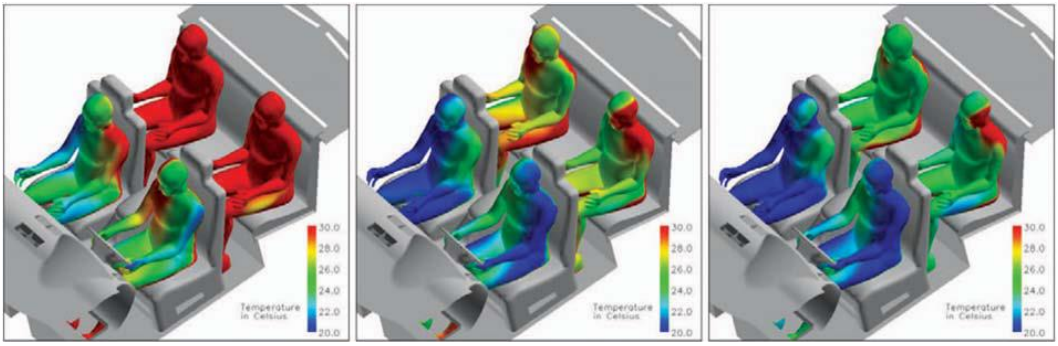

Figure 4. Results of climate control simulations in automobiles. Images courtesy of Visteon Corporation.

This application includes free shear flow near the vents, separation in the wake of the passengers and seats, near-wall turbulent thermal transport and thermal stratification. The Spalart-Allmaras model is successful at identifying the dominant flow features within the vehicle cabin and provides an acceptable prediction of the resulting thermal transport. Of course, the success of this application is dependent on the prediction of integrated engineering quantities, and not detailed point to point comparisons with experimental data. This class of problems is well validated in industry and simulations are regularly performed to design passenger comfort systems in lieu of extensive testing.

The preceding discussion is by no means a comprehensive review of the successes and downfalls of the Spalart-Allmaras model, or even RANS and URANS in general. The use of these modelling approaches for industrial applications are significant and could not be done justice by a single article. The next applications to be discussed involve a further increase in complexity, and are of great importance to current industrial efforts.

4.0 Current industrial demands

In this section, two CFD application areas are presented where the use of RANS and URANS is currently being investigated. These applications were chosen specifically due to the demands that they impose upon turbulence modelling technology.

4.1. Off-shore engineering applications

CFD analysis of off-shore engineering applications is becoming increasingly popular (Oakley et al. 2005, Constantinides and Oakley 2006, Constantinides et al. 2007, Holmes et

al. 2008). Simulations are necessary to reduce the cost and scope of expensive testing programs. Many of the applications of CFD in this field involve analysis of the effect of ocean currents and free surface waves on bluff geometries that are susceptible to complex fluid-structure interaction (FSI) phenomena such as vortex induced motion (VIM) and vortex induced vibration (VIV).

A schematic of a typical off-shore application, in this case an oil platform with spar and risers, is shown in **Figure 5a**. To illustrate the demands facing RANS modelling for off-shore applications, selected results from the validation efforts of a bare riser are presented.

The riser is the submerged cylindrical component of the platform that is shown in the lower portion of **Figure 5a**. A smooth-walled periodic section of the riser is modelled in the CFD simulation. **Figure 5b,c** display the results obtained from URANS and LES using the dynamic subgrid scale model at a Reynolds number of Re ¼ 1.4 6 105. The simulations were run on the same unstructured mesh consisting of 3.5 million elements (4-noded tetrahedra and 6-noded prisms). The model domain utilised periodic boundary conditions in the span, and had a span-wise length of 2Dh. **Table 2** shows the time averaged drag coefficient CD, the rms lift coefficient CL, and the Strouhal number St. Inspection of the results and comparison to various sources of experimental data (Cantwell and Coles 1983, Szepessy and Bearman 1992, West and Apelt 1993) reveal significant discrepancies among the modelling approaches.

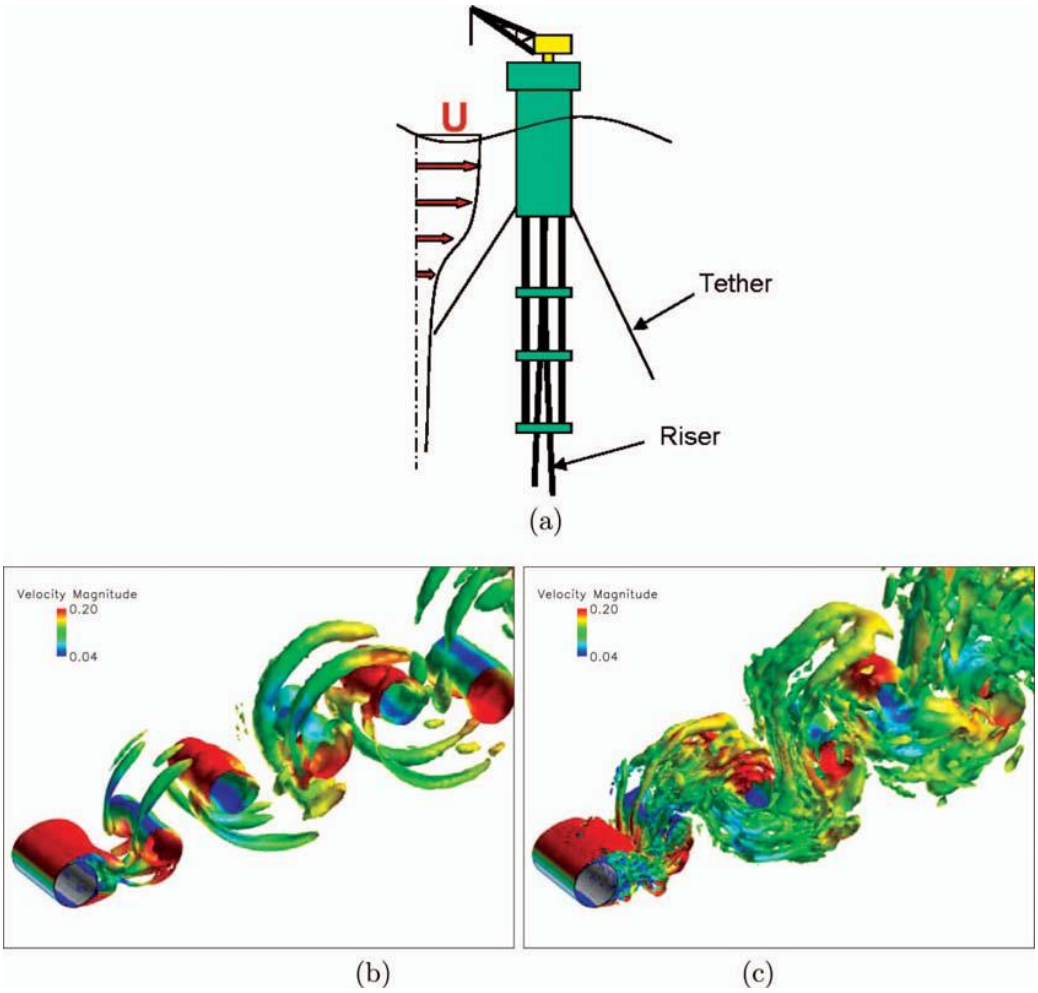

Figure 5. Off-shore industry applications: (a) schematic of oil platform with spar and risers; Iso-surfaces of $Q\left(-\frac{1}{2}\frac{\partial u_i}{\partial x_j}\frac{\partial u_j}{\partial x_i}\right)$ ***coloured by velocity magnitude (b) 3-D URANS; (c) LES simulation.***

	Cantwell & Coles	West & Apelt	Szepessy & Bearman	LES	URNAS	RANS
C_D	1.24	1.3	1.35	1.27	1.52	0.9
C_L, rms	–	0.58	0.5	0.58	1.16	–
St	0.18	–	–	0.2	0.21	–

Table 2. Comparison of RANS, URANS and LES results to experimental data.

The key result of this exercise is the difference in the mean flow field and drag coefficient predicted by each modelling approach. **Figure 6a** shows that the mean wake velocity predicted by the steady RANS solution has much lower velocities and a larger recirculation region. This is a clear example of an application where the flow is dominated by the large scale eddies that are difficult to account for in a steady RANS simulation. Focusing attention on the URANS results indicates some improvements in the wake closure length behind the body, as well as reasonable prediction of the Strouhal number. Despite these improvements over the steady RANS results, the URANS results over predict the lift and drag when compared to the experimental data and reference LES results.

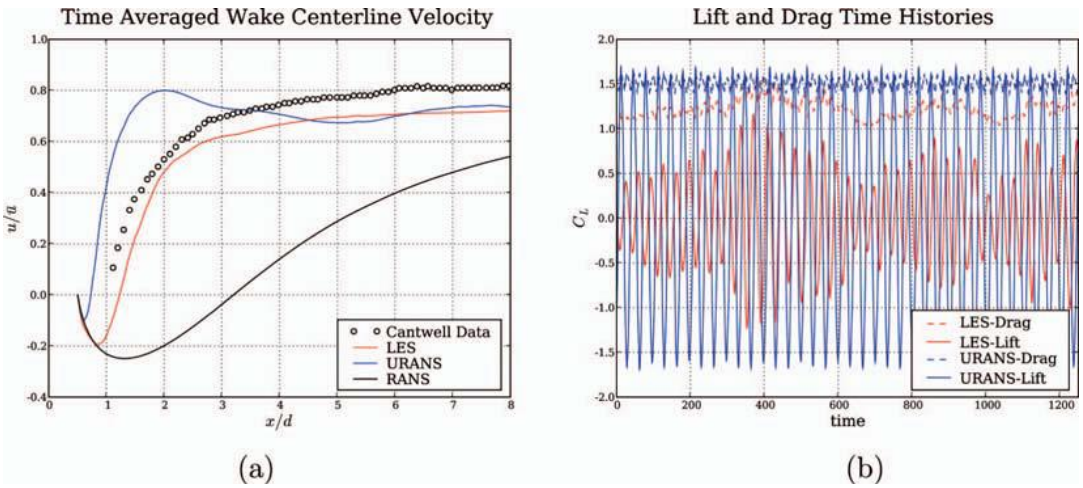

Figure 6. Results of riser simulations: (a) time averaged wake centreline velocity for RANS, URANS and LES, (b) fluctuating lift and drag coefficients.

The strong over prediction in magnitude of the fluctuating lift coefficient for the 3-D URANS case, shown in **Figure 6b** may be associated with the spanwise length of the domain. Similar behaviour was seen in the work of Shur et al. (2005). One other interesting result of the URANS is the presence of some three dimensional structure in the wake of the cylinder, as shown in **Figure 5b**. This figure qualitatively suggests that URANS is capable of resolving the threedimensionality of wake turbulence when considering two dimensional geometries on three dimensional meshes. The LES result shown in **Figure 5c**, however, produces a much larger degree of three-dimensionality in the wake region. Additionally, the LES result illustrates modulations in the lift coefficient that are reported in the experimental data. The URANS results do not reveal this detail of the lift fluctuations. The performance of the URANS model is consistent with the findings of others (Vaz et al. 2007) and this application illustrates a case where the current limitations of the RANS approach are reached. Significant improvements are needed to make this an attractive application area for RANS techniques.

4.2. Wind power applications

Renewable energy resources have gained a great deal of attention in recent years due to current economic factors. One of the renewable resources being pursued by many engineering organisations is the use of wind turbines to generate electrical power. The

applications of CFD in this industry are plentiful. The accuracy of the CFD is of great importance to provide turbine designs that are optimised not only for power generation, but also from a mechanical stand point to withstand loads induced by wind forces that give rise to FSI (i.e. blade flutter).

Consider the National Renewable Energy Laboratory (NREL) experiment consisting of a two-bladed wind turbine that utilised a twisted and tapered airfoil shape (Simms et al. 1999). In this illustration, the blades are assumed to be linearly elastic and the structural displacement is computed completely within AcuSolve based on the instantaneous wind loads. The blades are explicitly rotated at a constant rate of 72 RPM to resolve the interaction of the blade wake with the tower. **Figure 7a** shows the displacement of the blades resulting from the fluid forces, while **Figure 7b** gives an indication of the complex turbulent structure and separated flow in the wake of the blades.

Figure 7. URANS results at one time-step of NREL wind turbine simulation: (a) stream-wise displacement of wind turbine blades (undeformed shape shown in transparent grey); (b) iso-surfaces of Q coloured by velocity magnitude.

The wind turbine model was constructed as part of a technology demonstration exercise to illustrate the FSI capabilities of AcuSolve. The example is included in this discussion only to relay a sense of what industrial users are demanding of RANS and URANS modelling. Although no detailed experimental comparison of the blade displacement is available at this time, the results of a steady RANS investigation of the wind turbine rotor can be used to provide a rough indication of the expected level of accuracy for the forces on the blades.

Figure 8 indicates that the Spalart-Allmaras model does not accurately predict the change in flow behaviour as the wind speed increases. For the lower wind speed, the suction peak is over predicted, while it is significantly under predicted for the higher wind speed. To predict the time dependent loads on the blades, the separation size and shedding frequency must be simulated with reasonable accuracy. This places a large burden on the underlying RANS model, considering the transitional nature of the boundary layer and the extent of separation. Additionally, the current trend in the industry is towards larger turbine blades. This increases the required mesh size drastically, and makes DES and LES very expensive for this application.

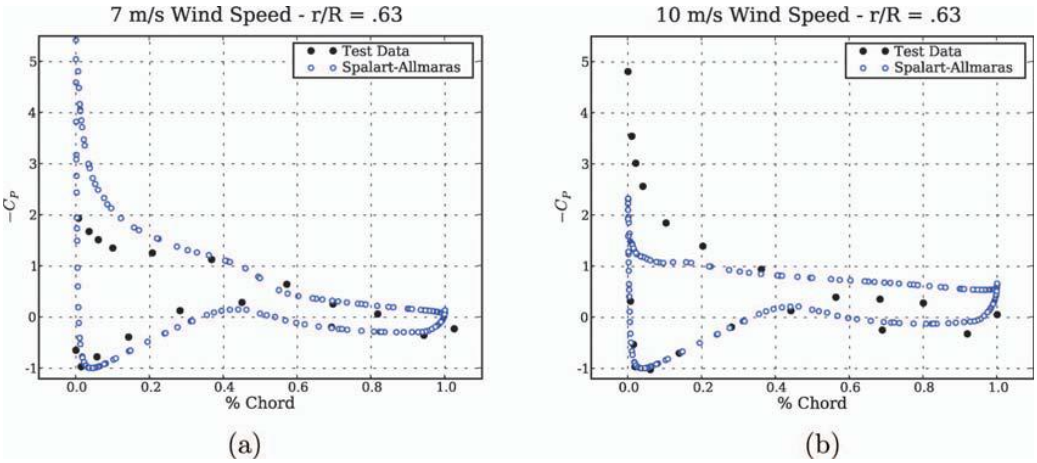

Figure 8. Steady RANS results showing pressure coefficient for NREL wind turbine blade at 63% rotor radius: (a) 7 m/s wind speed; (b) 10 m/s wind speed.

5.0 Discussion and future directions

The wind power and off-shore applications highlight four areas in which industrial users could benefit from improvements to RANS/URANS modelling technology. These areas can be characterised very broadly as; laminar-turbulent transition, massive separation, unsteady flow prediction and near wall modelling.

5.1. Laminar-turbulent transition

The flow over the oil platform riser and wind turbine blades both contain a complex combination of flow physics. Boundary layer transition plays a major role in accurately predicting the location of separation for both cases. Application of a correlation based transition model (Langtry and Menter 2005) to the flow over a cylinder (Langtry 2006) and a wind turbine blade (Langtry et al. 2006) using the SST RANS closure model showed improvements in results when compared to fully turbulent simulations. This approach to transition modelling appears very promising and it is hoped that continued experience with this methodology will lead to further advancements in this area and extension to other turbulence closures.

5.2. Massive separation

The results of the steady RANS model for the bare riser provides motivation for improvement of the RANS approach for bluff geometries and massively separated flows. It is acknowledged that the averaging technique utilised by steady RANS conflicts with the periodic shedding that characterises the flow over bluff bodies. However, the desire to rapidly produce predictions of drag on bluff industrial geometries remains strong. An accurate simulation of the drag crisis for a bare cylinder using a RANS closure, although tremendously difficult, would gain great attention by many industries and allow greater reliance on CFD in design processes.

5.3 Unsteady flow prediction

Unsteady simulations of flow over the oil platform riser and wind turbine are necessary to investigate FSI effects. CFD users are currently forced to choose from URANS, DES and LES as the turbulence modelling approach for these applications. For the bare riser, the URANS results were shown to provide an over prediction of the lift and drag forces. The LES model did improve the results significantly and provided a wealth of information about the turbulent structure in the wake. Unfortunately, this level of detail is not desired for the majority of industrial applications, and most users do not want to shoulder the expense of

running such simulations. Of greater interest to industrial users is a modelling approach that is 'smart' enough to determine what level of turbulent structures need to be resolved to validate the underlying assumptions of the model (i.e. the averaging operation). Ideally, this would be accomplished while avoiding grid dependant filtering operations. This yields a strong motivation to further investigate and develop URANS to provide better predictions for these types of simulations. The difficulty of accomplishing this within the RANS framework is understood, and it is possible that an altogether different approach needs to be pursued to achieve this.

5.4. Near wall modelling

Near wall modelling plays a large role in the use of RANS in industrial environments. It is not computationally efficient to explicitly resolve the near-wall activities for many high Reynolds number industrial applications. The applicability of wall functions for flows involving massive separation, transitional boundary layers and significant wall roughness needs to be further investigated. Development of reliable and accurate wall functions for these conditions would further improve the computational efficiency and ease of use of RANS modelling for industrial applications. Improvements to RANS modelling in the areas outlined above stand to provide great benefits to industrial users. The applications where these physics play a role extend far beyond the simulations that were discussed in this article. Excellent progress is already underway for incorporating transition modelling into RANS simulations. It is hoped that similar progress is made towards enabling better prediction of massively separated and unsteady flows while enabling users to employ wall models to reduce the cost of their RANS simulations.

6.0 Summary and conclusions

The ways in which industry successfully leverages the benefits of RANS modelling will continue to evolve as the applications of CFD increase. The characteristics that have established RANS as the dominant form of turbulence modelling in current practice help to solidify its importance for decades to come. Despite the successes of RANS, many current industrial applications expose limitations to the RANS modelling approach. For these applications, LES and DES provide a viable alternative at the expense of increased complexity and simulation time. However, considering the robustness, ease of use and efficiency of the RANS approach, researchers are encouraged to address these limitations directly within the RANS framework. The difficulty presented by this statement is understood, but it is also recognised that significant improvements to the capabilities of RANS modelling have been made in the recent past, and it is hoped that this article motivates researchers to focus their efforts and continue this progress in future years.

7.0 Acknowledgements

The authors thank Dr. L.J. Peltier and D. Lyons of Penn State's Applied Research Laboratory for their contribution of results, and Dr. Samuel H. Holmes for his helpful comments in improving the presentation of this article.

8.0 References

[1] Batten, P., Goldberg, U., and Chakravarthy, S., 2002. LNS -an approach towards embedded LES. AIAA. 2002 0427CP.

[2] Breuer, M., Jovicic, N., and Mazaev, K., 2003. Comparison of DES, RANS and LES for the separated flow around a flat plate at high incidence. International Journal For Numerical Methods in Fluids, 41, 357–388.

[3] Cantwell, B. and Coles, D., 1983. An experimental study of entrainment and transport in the turbulent near-wake of a circular cylinder. Journal of Fluid Mechanics, 136, 321–374.

[4] Carati, D., Jansen, K., and Lund, T., eds., 1995. Center for turbulence research annual research briefs. Stanford University/NASA Ames Research Center, Center for Turbulence Research, 35–40.

[5] Constantinides, Y. and Oakley, O., 2006. Numerical Prediction of Bare and Straked Cylinder VIV. Offshore Mechanics and Arctic Engineering OMAE2006-92334.

[6] Constantinides, Y., Oakley, O., and Holmes, S., 2007. CFD High L/D Riser Modeling Study. Offshore Mechanics and Arctic Engineering OMAE2007-29151 CP.

[7] Germano, M., et al., 1991. A dynamic subgrid-scale eddy viscosity model. Physics of Fluids A, 3, 1760–1765.

[8] Girimaji, D., Sreenivasan, R., and Jeong, E., 2003. PANS turbulence model for seamless transition between RANS, LES: fixed-point analysis and preliminary results. In: Proceedings of ASME FEDSM003 2003 4th ASMEJSME Joint Fluids Engineering Conference, Honolulu, HI, USA.

[9] Greenblatt, D., et al., 2004. A separation control CFD validation test case part 1: baseline and steady suction. 2nd AIAA Flow Control Conference, Portland, Oregon.

[10] Holmes, S., et al., 2008. Using CFD to study the effects of staggered buoyancy on drilling riser VIV. Offshore Mechanics and Arctic Engineering OMAE2008-57434 CP.

[11] Hughes, T., Mazzei, L., and Jansen, K., 2000. Large eddy simulation and the variational multiscale method. Computing and Visualization in Science, 3, 47–59.

[12] Hughes, T., Franca, L., and Hulbert, G., 1989. A new finite element formulation for computational fluid dynamics. VIII. The Galerkin/least-squares method for advective diffusive equations. Computer Methods in Applied Mechanics Engineering, 73, 173–189.

[13] Jansen, K.E., Whiting, C.H., and Hulbert, G.M., 2000. A generalized-a method for integrating the filtered Navier- Stokes equations with a stabilized finite element method. Computer Methods in Applied Mechanics Engineering, 190, 305–319.

[14] Langtry, R., 2006. A correlation-based transition model using local variables for unstructured parallelized CFD Codes. PhD Dissertation, University of Stuttgart.

[15] Langtry, R., Gola, J., and Menter, F., 2006. Predicting 2D Airfoil and 3D Wind Turbine Rotor Performance using a Transition Model for General CFD Codes. AIAA Aerospace Sciences Meeting and Exhibit, AIAA-2006-395.

[16] Langtry, R. and Menter, F., 2005. Transition Modelling for General CFD Applications in Aeronautics. AIAA Aerospace Sciences Meeting and Exhibit, AIAA-2005-522.

[17] Lyons, D., et al., 2007. Assessment of DES models for separated flow from a hump in a turbulent boundary layer. In: Proceedings of the Joint ASME/JSME Fluids Engineering Conference FEDSM 2007-37298, San Diego, CA, USA.

[18] Menter, F., Kuntz, M., and Bender, R., 2003. A Scale- Adaptive Simulation Model for Turbulent Flow Predictions. AIAA 2003-0767 CP.

[19] Moin, P., 1984. Probing turbulence via large eddy simulation. AIAA 84-0174 CP.

[20] Moin, P. and Kim, J., 1982. Numerical investigation of turbulent channel flows. Journal of Fluid Mechanics, 118, 341–377.

[21] Oakley, O., et al., 2005. Modeling Vortex Induced Motions of Spars in Uniform and Stratified Flows. Offshore Mechanics and Arctic Engineering OMAE2005-67238.

[22] Pope, S., ed., 2000. Turbulent Flows. 2nd ed. Cambridge:
Cambridge University Press.

[23] Samuel, A. and Joubert, P., 1974. A boundary layer developing in an increasingly adverse pressure gradient. Journal of Fluid Mechanics, 66, 481–505.

[24] Shakib, F., Hughes, T., and Johan, Z., 1991. A new finite element formulation for computational fluid dynamics. X. The compressible Euler and Navier-Stokes equations. Computer Methods in Applied Mechanics Engineering, 89, 141–219.

[25] Shur, M., et al., 2005. Three Dimensionality in Reynolds - Averaged Navier-Stokes Solutions Around Two-Dimensional Geometries. AIAA Journal, 43, 1230–1242.

[26] Simms, D., et al., 1999. Unsteady aerodynamics experiment phases II-IV test configurations and available data campaigns. NREL/TP-500-25950.

[27] Slimon, S., 2003. Computation of internal separated flows using a zonal detached eddy simulation approach. In: Proceedings of the 2003 ASME International Mechanical Engineering Congress, Washington D.C., USA.

[28] Smagorinsky, J., 1963. General circulation experiments with the primitive equations, i. the basic experiment. Monthly Weather Review, 91, 99–164.

[29] Spalart, P., 2000. Strategies for Turbulence Modelling and Simulations. International Journal of Heat and Fluid Flow, 21, 252–263.

[30] Spalart, P., et al., 2006. A New Version of Detached-Eddy Simulation, Resistant to Ambiguous Grid Densities. Journal of Theoretical and Computational Fluid Dynamics, 20, 181–195.

[31] Spalart, P., et al., 1997. Comments on the feasibility of LES for wings, and on a hybrid RANS/LES approach. In: C. Liu and Z. Liu, eds. Advances in DNS/LES. 137. Columbus, OH, USA: Greyden Press.

[32] Spalart, P. and Allmaras, S., 1992. A one-equation turbulence model for aerodynamic flows. AIAA 92-0439 CP.

[33] Szepessy, S. and Bearman, P., 1992. Aspect Ratio and End Plate Effects on Vortex Shedding from a Circular Cylinder. Journal of Fluid Mechanics, 234, 191–217.

[34] Vaz, G., Mabilat, C., Van Der Wal, R., and Gallagher, P., 2007. Viscous Flow Computations on Smooth Cylinders a Detailed Numerical Study With Validation. Offshore Mechanics and Arctic Engineering OMAE2007-29275.

[35] West, G. and Apelt, C., 1993. Measurement of Fluctuating Pressures and Forces on a Circular Cylinder in the Reynolds Number Range 10e4 to 2.5e5. Journal of Fluids and Structures, 7, 227–244.

[36] Wilcox, D., ed., 2000. Turbulence Modelling for CFD. 2nd ed. La Canada, CA: DCW Industries.